The mirtron miR-1010 functions in concert with its host gene SKIP to maintain synaptic homeostasis

Christopher Amourda[1,#] and Timothy E. Saunders[1,2,3,#]

[1] Mechanobiology Institute, National University of Singapore, Singapore
[2] Department of Biological Sciences, National University of Singapore, Singapore
[3] Institute of Molecular and Cell Biology, A*Star, Proteos, Singapore
[#] Correspondence: christopher.amourda@nus.edu.sg (lead contact) and dbsste@nus.edu.sg

Main text

MicroRNAs (miRNAs) are small non-coding RNAs that post-transcriptionally regulate gene expression in nearly all cellular pathways[1,2]. Recently, studies have revealed the existence of a non-canonical miRNA maturation pathway[3–5], whose miRNAs, named mirtrons, arise by splicing of an intron from a host gene[6]. A plethora of introns have been inferred as potential mirtrons[7–9], yet few have been experimentally validated and their functions, particularly in relation to their host genes, remain poorly understood[10,11]. Here, we show that the mirtron miR-1010 downregulates the nicotinic acetylcholine receptor β2 (nAcRβ2) and subsequently maintains synaptic homeostasis within an optimal range. We found that larvae lacking miR-1010 are unable to properly grow and pupariate. Increase of cortical nAcRβ2 mediated by neural activity elevates the level of intracellular calcium (Ca^{2+}). This high Ca^{2+} level activates the calcium/calmodulin-dependent kinase II (CaMKII) and, further downstream, the transcription factor Adf-1. We reveal that Adf-1 triggers the expression of SKIP, the host gene of miR-1010. SKIP tempers synaptic potential by regulating Shal, a potassium voltage-gated channel protein. MiR-1010 reduces the mRNA level of nAcRβ2 to prevent synaptic potentials from overshooting their optimal range. Our results demonstrate how a mirtron, in concert with its host gene, contributes to maintaining homeostasis.

Since their discovery more than two decades ago[12,13], miRNAs have been established as key cellular micromanagers. Canonical miRNAs are genetically encoded short (18-22 nucleotides) hairpin structures that are processed, after transcription, by the Drosha/Pasha

pathway[6]. They are subsequently exported from the nucleus and undergo a final step of maturation before being functionally able to regulate the mRNA level of their target genes[2,14,15]. Mirtrons were identified as a non-canonical miRNA maturation pathway in which introns are debranched from precursor mRNAs and enter the miRNA processing pathway without requiring cleavage by Drosha[3,4]. Mirtrons are widespread across taxa and some show a high degree of conservation[10], implying important regulatory functions. Nevertheless, their functions and the reason for their emergence within introns remain elusive.

We brought our attention to the mirtron miR-1010 as homozygous mutants are lethal[16]. MiR-1010 is located within the Shal potassium (K^+) channel Interacting Protein (SKIP), between exons 4 and 5 (Fig. 1a and Supplementary Fig. S1). Replacing miR-1010 by a LoxP sequence does not affect embryogenesis as larvae hatch without any apparent defects and with similar viability as wild-type animals. However, mutant larvae are unable to grow; they retain a first instar larva size (<0.5mg) and fail to pupariate (Fig. 1b). The ecdysone pathway, a steroid hormone controlling larval moulting[17,18], appears unaffected (Supplementary Fig. S2a-e) whereas the insulin receptor (dInr) and the *Drosophila* insulin-like peptide 2 (Dilp2) are upregulated to counteract the lack of growth (Supplementary Fig. S2f-g). The standard level of chico (substrate of the insulin receptor[19]), sNPF and ns3 (both involved in dilp2 secretion[19]) concur with the insulin pathway and dilp2 secretion being operative in miR-1010$^{-/-}$ (Supplementary Fig. S2h-j). Moreover, we observed no defect in food intake in miR-1010$^{-/-}$ larvae (Fig. 1c). Strikingly, the metabolic brake[20], 4E-BP, shows a 10-fold increase directly at the onset of larval life in miR-1010 mutants as compared to wild-type larvae (Fig. 1d). The high level of 4E-BP indicates that larvae sense a stressful condition and, as a result, growth is inhibited until returning to adequate condition[20]. To understand the causes underlying the miR-1010$^{-/-}$ phenotype, we first sought to verify that the impeded growth is solely due to the lack of miR-1010 and not a result of an alteration of SKIP. We used a SKIP MiMIC (SKIP$^{-/-}$) mutant where a triple stop codon is inserted within the first intron[21]. Importantly, the MiMIC

insertion does not prevent transcription but alters the translation of a given gene. Hence, the miR-1010 level remains at a wild-type level in SKIP$^{-/-}$ larvae (Supplementary Fig. S2k). Concordantly, SKIP$^{-/-}$ larvae show a mild timing phenotype and pupate with a 24h delay (Fig. 1b). These results indicate that the deficit in larval growth is due to a lack of miR-1010.

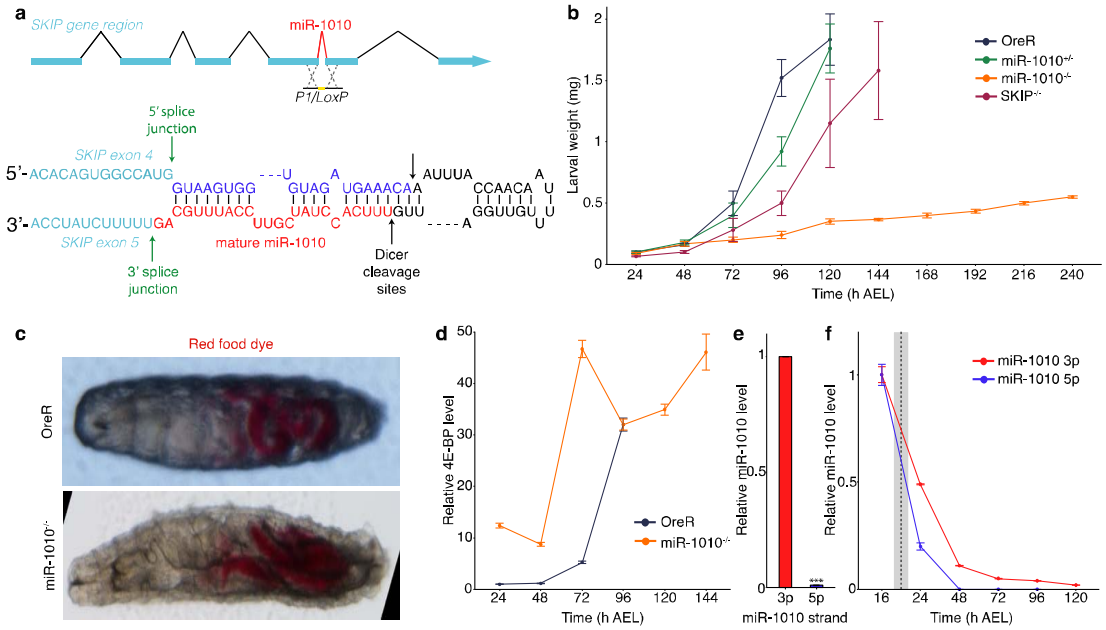

Fig 1 | Larvae fail to grow and pupariate in miR-1010$^{-/-}$. (**a**) The mirtron miR-1010 is located in the SKIP gene, between the exons 4 and 5. The entire miR-1010 has been replaced by a LoxP sequence in the miR-1010$^{-/-}$ line (top panel). MiR-1010 forms a hairpin loop and is debranched from SKIP by the splicing machinery and further matures as a normal miRNA (bottom panel). (**b**) Larval weight was measured directly after hatching until pupariation. OreR, miR-1010$^{+/-}$ and SKIP$^{-/-}$ reached ~2mg before pupariation. MiR-1010$^{-/-}$ weight was recorded for 10 days but did not pupariate. (**c**) Stereoscope pictures of OreR and miR-1010$^{-/-}$ larvae allowed to eat coloured yeast paste show no feeding behaviour defect. (**d**) Larval 4E-BP transcript levels measured by RT-qPCR in OreR and miR-1010$^{-/-}$. Fold changes are relative to OreR at 24h AEL. (**e-f**) MiR-1010 strand specific RT-qPCR shows a strong bias toward miR-1010 3p (**e**) and a high expression during embryogenesis before gradually decreasing during larval stages (**f**). Expression level are relative to the expression at 16h AEL. The dashed line indicates the average hatching time and the grey rectangle represents the standard deviation in hatching times at 25ºC. All values are means ± SD (***P<0.001, n = at least 9 for each experiment).

We next sought to identify the targets of miR-1010. In contrast to canonical miRNAs, mirtrons 3' arms are preferentially more stable than their 5' complement[4]. Consistent with the biased stability, we found only traces of miR-1010 5' strand throughout development (Fig. 1e). Further, we observed that miR-1010 has its highest expression during mid-embryogenesis

(16h AEL) and gradually decreases during larval development (Fig. 1f). We next used a Gal4 driver inserted downstream of the SKIP regulatory region to locate the spatial expression of both SKIP and miR-1010. We assume here that SKIP and miR-1010 have the same expression pattern as miR-1010 arises from the debranching of SKIP introns. We found that SKIP and miR-1010 are expressed in the central nervous system (CNS) and more prominently in the axons emanating from the CNS (Fig. 2a and Movie 1). Coupling this expression pattern with the computationally predicted targets[3,22–24] for the miR-1010 3' strand, we refined a list of targets and examined their expression in miR-1010$^{-/-}$. Amongst 36 tested targets, we found that Drl-2, nAcRβ2 and CG3078 are (i) expressed at meaningful level (judged by the Ct values in qPCR experiments) and (ii) consistently overexpressed (generally >2-fold for all targets) in miR-1010$^{-/-}$ throughout larval development (Fig. 2b-d and Supplementary Fig. S3a). Of these, only nAcRβ2 shows higher expression during embryogenesis (Supplementary Fig. S3b). Notably, the nAcRβ2 is amongst the most prominently expressed nAcRs during early larval life and further the only subtype overexpressed in miR-1010$^{-/-}$ (Supplementary Fig. S3c-d). We infer from these data that nAcRβ2 plays a crucial role at this stage of development and accounts, in part, for the phenotype observed in miR-1010$^{-/-}$. Alongside the predicted targets, we noticed that the mRNA levels of SKIP and Shal in miR-1010$^{-/-}$ larvae shows a ~3-fold increase as compared to control larvae (Fig. 2e). The increase in mRNA level translates into an increase in protein level for both nAcRβ2 and SKIP (Supplementary Fig. S3e-f). Importantly, the nAcRβ2 protein level is slightly increased during embryogenesis but dramatically greater at larval stages in miR-1010$^{-/-}$ (Supplementary Fig. S3e). SKIP has two shorter isoforms besides its full length protein[25] and we observed an upregulation of both the full length and the SKIP3 isoforms at larval stages (Supplementary Fig. S3f). These results suggest that miR-1010, its host gene, and targets are within the same regulatory pathway.

We next attempted to rescue the miR-1010$^{-/-}$ phenotype by knocking down specific targets. Mutants for Drl-2 and CG3078 fail to rescue the miR-1010$^{-/-}$ phenotype (Supplementary Fig. S4a). We were unable to perform similar rescue experiment for the nAcRβ2 as the cytogenic locations of miR-1010 and nAcRβ2 are in close proximity (94A4 and 96A5, respectively) and therefore prevent chromosomal recombination. MiRNA deficiency essentially results in overexpression of its targets. We reasoned that overexpressing the coding sequence (i.e. without the 3'UTR bearing miR-1010 binding sites) should phenocopy miR-1010$^{-/-}$ (Supplementary Fig. S4b). We did not impede larval growth as in miR-1010$^{-/-}$ (Supplementary Fig. S4c-e), nevertheless, pan-neural (Elav>Gal4) overexpression of nAcRβ2 resulted in an interesting pattern whereby SKIP, miR-1010 and Shal are upregulated along with Drl-2 and CG3078 (Fig. 2f). On the contrary, overexpression of nAcRβ2 in sensory neurons using Pickpocket Gal4 driver[26,27] (ppk>Gal4) does not increase the level of SKIP, miR-1010 and Shal (Fig. 2f). These results indicate that miR-1010 is neuron specific. Overexpressing Drl-2 or CG3078 with Elav>Gal4 does not affect the levels of nAcRβ2, SKIP and Shal (Supplementary Fig. S4f-g). Further, we noticed that the SKIP>Gal4 driver line (when homozygous) exhibits a high level of nAcRβ2 accompanied by high levels of SKIP and Shal (Fig. 2g). The SKIP>Gal4 line is, however, homozygous viable. Therefore, this expression pattern indicates that SKIP transcription or introns debranching is sub-optimal in the SKIP>Gal4 line. This phenotype can be partially rescued upon restoring a copy of a wild-type chromosome (Fig. 2g). Last, we were able to rescue the larval growth defects in miR-1010$^{-/-}$ by expressing miR-1010 under the pan-neural driver Elav (Fig. 2h and Supplementary Fig. S4h-j). The mRNA levels of nAcRβ2, Shal, Drl-2 and CG3078 are brought down by the overexpression of miR-1010. However, SKIP level is consistently higher (~10-fold) in the rescue line. This expression pattern is surprising and further experiments will be required to understand the reason underlying SKIP upregulation.

Altogether, these experiments indicate that increase in nAcRβ2 gives rise to an upregulation of SKIP, miR-1010 and Shal genes, a necessity to maintain the neural circuit under adequate condition. The upregulation of Drl-2 and CG3078 upon nAcRβ2 increase is intriguing. The most likely explanation is that the higher levels of Drl-2 and CG3078 in miR-1010$^{-/-}$ larvae is simply a response to increased neural activity, not the direct result of a lack of miR-1010. CG3078 upregulation upon neural activity is plausible as its inferred function is to regulate K^+ channel activity[28]. However, the reason for Drl-2, an axon guiding protein[29–31], upregulation is more enigmatic and may be a response to axonal growth following increased activity.

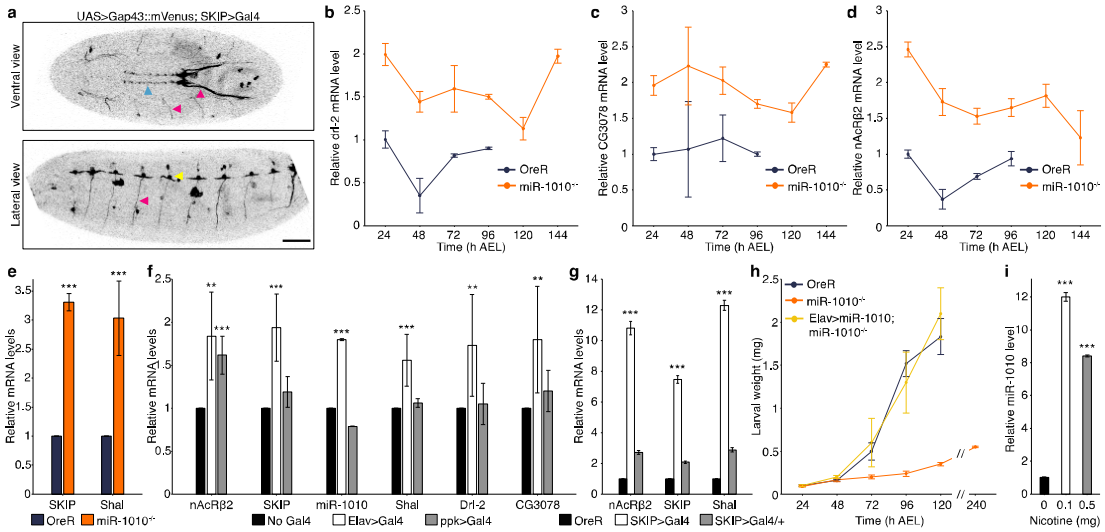

Fig 2 | nAcRβ2, Drl-2 and CG3078 levels is elevated in miR-1010$^{-/-}$ (**a**) Confocal imaging of embryos expressing a membrane marker (UAS>Gap43::mVenus) driven by SKIP>Gal4. SKIP/miR-1010 are expressed in the CNS (blue arrowhead), in axons (pink arrowheads) emanating from the CNS and at neuromuscular junctions (yellow arrowhead). Scale bar is 50µm. (**b-d**) Drl-2 (**b**), CG3078 (**c**) and nAcRβ2 (**d**) transcript levels (RT-qPCR) in miR-1010$^{-/-}$ (orange). Fold changes are relative to OreR (dark blue) at 24h AEL. (**e**) SKIP and Shal transcript levels (RT-qPCR) in miR-1010$^{-/-}$ relative to OreR larvae at 24h AEL. (**f**) Transcripts levels (RT-qPCR) in nAcRβ2 overexpressed by Elav>Gal4 (white) or ppk>Gal4 (grey) relative to non-induce UAS>nAcRβ2 (black) at 24h AEL. (**g**) nAcRβ2, SKIP and Shal transcript levels (RT-qPCR) in homozygous SKIP>Gal4 (white) and in SKIP>Gal4/+ (gray) relative to OreR (black) at 24h AEL. (**h**) Larval weight was measured in OreR, miR-1010$^{-/-}$ and in Elav>Gal4/UAS>miR-1010; miR-1010$^{-/-}$ rescue line. (**i**) miR-1010 levels upon exposure to 0.1mg (white) and 0.5mg (gray) of nicotine as compared to 0mg (black). All values are means ± SD (*P<0.05, **P<0.01, ***P<0.001, n = at least 9 for each experiment).

Ping and Tsunoda[32] recently demonstrated that nAcRs boost synaptic potentials and trigger the upregulation of cortical nAcRs. These receptors are permeable to Ca^{2+} and the subsequent influx of Ca^{2+} activates the CaMKII. In turn, CaMKII triggers the expression of the Shal K^+ channel. Therefore, K^+ ions are released from neurons and temper membrane potentials. Whilst homeostatic mechanisms to compensate loss in membrane potentials have been broadly studied, the authors revealed the existence of a pathway required to stabilise synaptic potentials. Despite the apparent importance of such a pathway, we found that neither knockdowns of Shal nor its first interactor SKIP, resulted in lethality (Supplementary Fig. S4k). Combining these results, we hypothesised that the mRNA level of nAcRβ2 is downregulated by miR-1010 and that this negative feedback works complementarily to SKIP and Shal to temper synaptic potentials. As previously described, SKIP is presumed to modulate Shal channels inactivation kinetic[25,33,34]. To corroborate our model, we exposed wild-type larvae to different doses (0.1 and 0.5mg) of nicotine, agonist of nAcRs, for 24h. We saw a striking ~10-fold increase in miR-1010 level for both dosage conditions (Fig. 2i). This result shows that there exists a direct relationship between nAcRs activation and miR-1010 expression.

We next examined the regulation of SKIP and Shal expression. Through computational analysis, we found that the transcription factor Adf-1 has predicted binding sequences in both Shal and SKIP regulatory regions[35,36] (Supplementary Fig. S5a). Further, Adf-1 is phosphorylated by CaMKII and is therefore a plausible candidate[37]. It has also been demonstrated by ChIP-seq experiments that Adf-1 is phosphorylated upon neural activity and blocks Fas2 and (indirectly) Staufen to allow neuronal growth[37]. We obtained the ChIP-seq results mentioned above and noticed that Adf-1 also binds to Shal and to a smaller extent to SKIP (Supplementary Fig. S5b). We confirmed these results by performing a ChIP-qPCR for Adf-1 and showed that Adf-1 strongly binds Fas2, Shal and SKIP regulatory regions in OreR and miR-1010$^{+/-}$ mutants. However, this binding is significantly reduced in miR-1010$^{-/-}$ (Fig.

3a). Adf-1 has been shown to positively correlate with high Pol II-pausing indices[37]. Therefore, we reasoned that in its non-phosphorylated state Adf-1 is bound to Shal and SKIP regulatory elements and prevents their transcription. Upon neural activity, Adf-1 is phosphorylated and releases Shal and SKIP expression. If our hypothesis is correct, we should then observe higher levels of SKIP, miR-1010 and Shal in Adf-1$^{-/-}$ larvae. The majority of Adf-1$^{-/-}$ (~80%) fail to complete embryogenesis[38]. Those that survive to larval stages do not noticeably grow and display a phenotype reminiscent to that of miR-1010$^{-/-}$ larvae (Fig. 3b). We performed qPCR on Adf-1$^{-/-}$ that reached the larval stage and we saw a general increase in mRNA levels for all candidates (Fig. 3c). However, our results are quite variable, a phenomenon unsurprising given the pleiotropic function of Adf-1[37,38]. Adf-1 promotes neuronal growth upon neural activity by shutting down Fas2 and Staufen. However, mechanism(s) must be in place to prevent detrimental overgrowth. By having Adf-1 also regulate Shal and SKIP, the system couples growth to neural activity. This mechanism introduces an incoherent feedforward loop to ensure robust growth in response to neural activity (Fig. 3d).

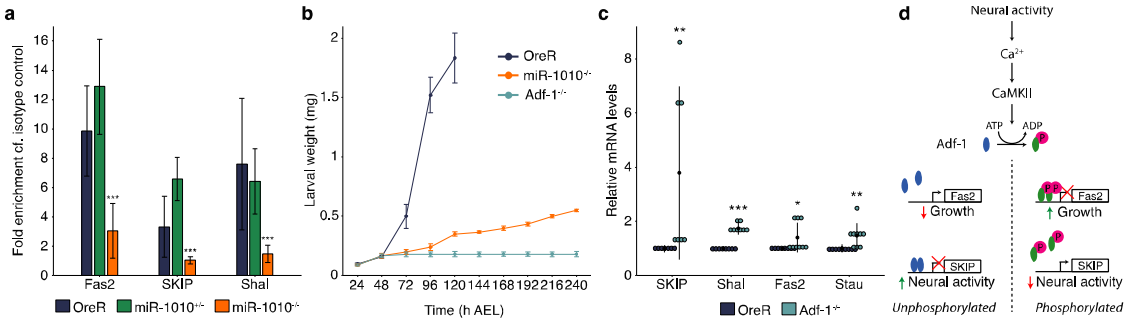

Fig 3 | Adf-1 controls the expression of SKIP, miR-1010 and Shal. (**a**) ChIP-qPCR for Adf-1 performed in OreR (darkblue), miR-1010$^{+/-}$ (green) and miR-1010$^{-/-}$ (orange). Fold enrichments are relative to the Rabbit IgG isotype control. (**b**) Larval weight in Adf-1$^{-/-}$ as compared to OreR and miR-1010$^{-/-}$. (**c**) Dot plot representing transcript levels measured in Adf-1$^{-/-}$ (turquoise) relative to OreR (dark blue) at 24h AEL. Black dots and lines represent, respectively, the mean and the standard deviation for each condition. (**d**) Model of Adf-1-mediated coupling of neural activity and growth. Adf-1 is represented in blue in its non-phosphorylated form and in green upon phosphorylation. All values are means ± SD (*P<0.05, **P<0.01, ***P<0.001, n = at least 9 for each experiments).

We have revealed here nAcRβ2, Shal, SKIP and miR-1010 form a network that contains an incoherent feedforward loop coupled with a negative feedback loop (Fig. 4a). Therefore, the mirtron miR-1010 and its host gene SKIP appear to work in tandem to ensure synaptic homeostasis (Fig. 4b). To test this conclusion, we used mass-action kinetics to model the average long-term voltage potential response due to the two interaction loops outlined in Fig. 4a after activation of nAcRβ2 (see Supplementary Note for details). We see that loss of SKIP or partial loss of miR-1010 results in delayed return of the potential to homeostatic levels (Fig. 4c), consistent with our observed delay in developmental time (Fig. 1b). However, complete loss of miR-1010 results in the potential staying active over a long period (Fig. 4c), consistent with the observed stress response seen in miR-1010$^{-/-}$. The modelling reveals that miR-1010 is effectively acting like a switch, controlling whether nAcRβ2 has high or low expression, and this switch-like behaviour is dependent on miR-1010 expression levels (see Supplementary Note for further discussion). The model predicts that the average membrane potential response will also be higher in miR-1010$^{+/-}$ and SKIP$^{-/-}$ and it will be interesting to test this, for example using a GCaMP reporter.

We have studied the role of miR-1010 in a developmental context but it is important to note that exposure to nicotine results in a dramatic increase of miR-1010 level in wild-type larvae. Hence, this pathway is likely not restricted to development and applies to later stages of life. Besides shedding light onto the coherence between the functions of mirtrons and their host genes, we predict that miR-1010 (and its mammalian orthologue) plays an important role in nicotine-related diseases.

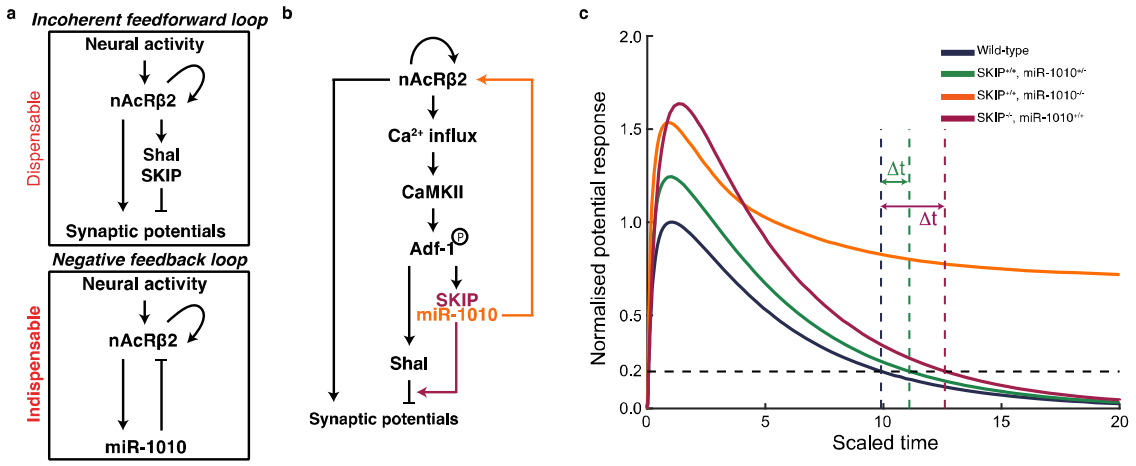

Fig 4 | miR-1010 controls synaptic homeostasis by downregulating nAcRβ2. (**a**) nAcRβ2 is part of incoherent feedforward loop to temper synaptic potentials and a negative feedback loop through which miR-1010 downregulates nAcRβ2 upon receptor activation. (**b**) Both loops work cooperatively to prevent synaptic potentials from overshooting their optimal range. (**c**) Long-term average potential response obtained by mass-action kinetic simulation of model outlined in (**a**). Resting potential defined to 0 (corresponding to ~-70meV). Curves normalised to maximum potential in wild-type simulation (parameters and description in Supplementary Note). Time is scaled relative to the lifetime of nAcRβ2. Δt represents delay in potential in miR-1010$^{+/-}$ and SKIP$^{-/-}$ to return to less than 20% of peak response in wild-type conditions.

Acknowledgments:

We thank Victor Corces and Stephen Cohen for sharing precious reagents and data. We acknowledge Katsutomo Okamura and all Saunders' lab members for fruitful discussions. This work was supported by the National Research Foundation Singapore under an NRF Fellowship to T.E.S. (NRF2012NRF-NRFF001-094).

Author Contributions:

C.A. designed the study, performed the experiments, analysed the data and wrote the manuscript. T.E.S. performed the mathematical modelling, aided in the study design and statistical analysis, and contributed to writing the manuscript. Both authors agree to the final version of the manuscript.

The authors declare no competing financial interest.

References

1. Pasquinelli, A. E., Hunter, S. & Bracht, J. MicroRNAs: A developing story. *Curr. Opin. Genet. Dev.* **15,** 200–205 (2005).

2. Carthew, R. W., Agbu, P. & Giri, R. MicroRNA function in Drosophila melanogaster. *Semin. Cell Dev. Biol.* **65,** 29–37 (2017).

3. Ruby, J. G., Jan, C. H. & Bartel, D. P. Intronic microRNA precursors that bypass Drosha processing. *Nature* **448,** 83–86 (2007).

4. Okamura, K., Hagen, J. W., Duan, H., Tyler, D. M. & Lai, E. C. The Mirtron Pathway Generates microRNA-Class Regulatory RNAs in Drosophila. *Cell* **130,** 89–100 (2007).

5. Westholm, J. O. & Lai, E. C. Mirtrons: MicroRNA biogenesis via splicing. *Biochimie* **93,** 1897–1904 (2011).

6. Berezikov, E. Evolution of microRNA diversity and regulation in animals. *Nat. Rev. Genet.* **12,** 846–60 (2011).

7. Chung, W. *et al.* Computational and experimental identification of mirtrons in Drosophila melanogaster and Caenorhabditis elegans. *Genome Res.* **21,** 286–300 (2011).

8. Wen, J., Ladewig, E., Shenker, S., Mohammed, J. & Lai, E. C. Analysis of Nearly One Thousand Mammalian Mirtrons Reveals Novel Features of Dicer Substrates. *PLoS Comput. Biol.* **11,** e1004441 (2015).

9. Ladewig, E., Okamura, K., Flynt, A. S., Westholm, J. O. & Lai, E. C. Discovery of hundreds of mirtrons in mouse and human small RNA data. *Genome Res.* **22,** 1634–1645 (2012).

10. Curtis, H. J., Sibley, C. R. & Wood, M. J. A. Mirtrons, an emerging class of atypical miRNA. *Wiley Interdiscip. Rev. RNA* **3,** 617–632 (2012).

11. Inui, M. *et al.* Dissecting the roles of miR-140 and its host gene. *Nat. Cell Biol.* **20,** 516–518 (2018).

12. Lee, R. C., Feinbaum, R. L. & Ambros, V. The C . elegans Heterochronic Gene lin-4 Encodes Small RNAs with Antisense Complementarity to & II-14. *Cell* **75,** 843–854 (1993).

13. Wightman, B., Ha, I. & Ruvkun, G. Posttranscriptional regulation of the heterochronic gene lin-14 by lin-4 mediates temporal pattern formation in C. elegans. *Cell* **75,** 855–862 (1993).

14. Giri, R. & Carthew, R. W. microRNAs suppress cellular phenotypic heterogeneity. *Cell Cycle* **13,** 1517–1518 (2014).

15. Chandra, S. *et al.* Role of miRNAs in development and disease: Lessons learnt from small organisms. *Life Sci.* **185,** 8–14 (2017).

16. Chen, Y. *et al.* Resource Systematic Study of Drosophila MicroRNA Functions Using

a Collection of Targeted Knockout Mutations. *Dev. Cell* **31,** 784–800 (2014).

17. Baehrecke, E. H. Ecdysone signaling cascade and regulation of Drosophila metamorphosis. *Arch. Insect Biochem. Physiol.* **33,** 231–44 (1996).

18. Yamanaka, N., Rewitz, K. F. & O'Connor, M. B. Ecdysone Control of Developmental Transitions: Lessons from *Drosophila* Research. *Annu. Rev. Entomol.* **58,** 497–516 (2013).

19. Boulan, L., Milán, M. & Léoplold, P. The Systemic Control of Growth. *Cold Spring Harb. Perspect. Biol.* **7,** a019117 (2016).

20. Teleman, A. A., Chen, Y. W. & Cohen, S. M. 4E-BP functions as a metabolic brake used under stress conditions but not during normal growth. *Genes Dev.* **19,** 1844–1848 (2005).

21. Venken, K. J. T. *et al.* MiMIC: a highly versatile transposon insertion resource for engineering Drosophila melanogaster genes. *Nat. Methods* **8,** 737–743 (2011).

22. Ruby, J. G. *et al.* Evolution, biogenesis, expression, and target predictions of a substantially expanded set of Drosophila microRNAs. *Genome Res.* **17,** 1850–1864 (2007).

23. Kheradpour, P., Stark, A., Roy, S. & Kellis, M. Reliable prediction of regulator targets using 12 Drosophila genomes. *Genome Res.* **17,** 1919–1931 (2007).

24. Lewis, B. P., Burge, C. B. & Bartel, D. P. Conserved seed pairing, often flanked by adenosines, indicates that thousands of human genes are microRNA targets. *Cell* **120,** 15–20 (2005).

25. Diao, F., Waro, G. & Tsunoda, S. Fast inactivation of Shal (Kv4) K+ channels is regulated by the novel interactor SKIP3 in Drosophila neurons. *Mol. Cell. Neurosci.* **42,** 33–44 (2009).

26. Adams, C. M. *et al.* Ripped Pocket and Pickpocket, Novel Drosophila DEG/ENaC Subunits Expressed in Early Development and in Mechanosensory Neurons. *J. Cell Biol.* **140,** 143–152 (1998).

27. Ainsley, J. A., Kim, M. J., Wegman, L. J., Pettus, J. M. & Johnson, W. A. Sensory mechanisms controlling the timing of larval developmental and behavioral transitions require the Drosophila DEG/ENaC subunit, Pickpocket1. *Dev. Biol.* **322,** 46–55 (2008).

28. Gramates, L. S. *et al.* FlyBase at 25: Looking to the future. *Nucleic Acids Res.* **45,** D663–D671 (2017).

29. Reynaud, E. *et al.* Guidance of Drosophila Mushroom Body Axons Depends upon DRL-Wnt Receptor Cleavage in the Brain Dorsomedial Lineage Precursors. *Cell Rep.* **11,** 1293–1304 (2015).

30. Grillenzoni, N., Flandre, A., Lasbleiz, C. & Dura, J.-M. Respective roles of the DRL receptor and its ligand WNT5 in Drosophila mushroom body development. *Development* **134,** 3089–3097 (2007).

31. Sakurai, M. *et al.* Differentially Expressed Drl and Drl-2 Play Opposing Roles in Wnt5 Signaling during Drosophila Olfactory System Development. *J. Neurosci.* **29,** 4972–4980 (2009).

32. Ping, Y. & Tsunoda, S. Inactivity-induced increase in nAChRs upregulates Shal K+ channels to stabilize synaptic potentials. *Nat. Neurosci.* **15,** 90–97 (2011).

33. Tsunoda, S. & Salkoff, L. Genetic analysis of Drosophila neurons: Shal, Shaw, and Shab encode most embryonic potassium currents. *J. Neurosci.* **15,** 1741–1754 (1995).

34. Ping, Y. *et al.* Shal/Kv4 channels are required for maintaining excitability during repetitive firing and normal locomotion in Drosophila. *PLoS One* **6,** 15–20 (2011).

35. Messeguer, X. *et al.* PROMO: Detection of known transcription regulatory elements using species-tailored searches. *Bioinformatics* **18,** 333–334 (2002).

36. Farré, D. *et al.* Identification of patterns in biological sequences at the ALGGEN server: PROMO and MALGEN. *Nucleic Acids Res.* **31,** 3651–3653 (2003).

37. Timmerman, C. *et al.* The Drosophila Transcription Factor Adf-1 (nalyot) Regulates Dendrite Growth by Controlling FasII and Staufen Expression Downstream of CaMKII and Neural Activity. *J. Neurosci.* **33,** 11916–11931 (2013).

38. Dezazzo, J. *et al.* nalyot , a Mutation of the Drosophila Myb-Related Adf1 Transcription Factor , Disrupts Synapse Formation and Olfactory Memory. *Neuron* **27,** 145–158 (2000).